EBioMedicine
Published by THE LANCET

Research paper

A novel mechanism of synaptic and cognitive impairments mediated via microRNA-30b in Alzheimer's disease

Yunping Song [a,1], Mei Hu [a,2], Jian Zhang [a], Zhao-qian Teng [a,3], Chu Chen [a,b,*]

[a] Neuroscience Center of Excellence, Louisiana State University Health Sciences Center, New Orleans, LA 70112, USA
[b] Department of Otorhinolaryngology, Louisiana State University Health Sciences Center, New Orleans, LA 70112, USA

ARTICLE INFO

ABSTRACT

Background: It is widely accepted that cognitive and memory deficits in Alzheimer's disease (AD) primarily result from synaptic failure. However, the mechanisms that underlie synaptic and cognitive dysfunction remain unclear.

Methods: We utilized molecular biology techniques, electrophysiological recordings, fluorescence in situ hybridization (FISH), immuno- and Golgi-staining, chromatin immunoprecipitation (CHIP); lentivirus (LV)-based microRNA overexpression and 'sponging', and behavioral tests to assess upregulated miR-30b causing synaptic and cognitive declines in APP transgenic (TG) mice.

Findings: We provide evidence that expression of miR-30b, which targets molecules important for maintaining synaptic integrity, including ephrin type-B receptor 2 (ephB2), sirtuin1 (sirt1), and glutamate ionotropic receptor AMPA type subunit 2 (GluA2), is robustly upregulated in the brains of both AD patients and APP transgenic (TG) mice, an animal model of AD, while expression of its targets is significantly downregulated. Overexpression of miR-30b in the hippocampus of normal wild-type (WT) mice impairs synaptic and cognitive functions, mimicking those seen in TG mice. Conversely, knockdown of endogenous miR-30b in TG mice prevents synaptic and cognitive decline. We further observed that expression of miR-30b is upregulated by proinflammatory cytokines and Aβ42 through NF-κB signaling.

Interpretation: Our results provide a previously undefined mechanism by which unregulated miR-30b causes synaptic and cognitive dysfunction in AD, suggesting that reversal of dysregulated miR-30b in the brain may prevent or slow cognitive declines in AD.

Fund: This work was supported by National Institutes of Health grants R01NS076815, R01MH113535, R01AG058621, P30GM103340 Pilot Project, and by the LSUHSC School of Medicine Research Enhancement Program grant (to C.C.).

1. Introduction

Alzheimer's disease (AD) is the most common cause of dementia in the elderly. Unfortunately, largely due to our limited understanding of the mechanisms involved in the pathogenesis and neuropathology of AD, there are no effective therapies to prevent development of AD or to halt disease progression.

The most important consequences of neuropathological changes, including extracellular deposition of β-amyloid (Aβ) plaques and accumulation of soluble Aβ, intracellular formation of hyperphosphorylated tau proteins, and chronic neuroinflammation, are synaptic malfunction and/or loss of synapses, which eventually lead to neurodegeneration, loss of memory, and dementia in AD. Although the etiology of AD is multifactorial and complex, it is generally accepted that cognitive and memory deficits in AD at early stages primarily result from synaptic failure [1–4]. However, the mechanisms that underlie synaptic dysfunction remain unclear. The human brain contains >100 billion nerve cells that are connected by >1000 trillion synapses through which signals are transmitted from one neuron to another, indicating that optimal synaptic communications in the brain are fundamental for normal physiological function

---

* Corresponding author at: Neuroscience Center of Excellence, School of Medicine, Louisiana State University Health Sciences Center, 2020 Gravier Street, Suite D, New Orleans, LA 70112, USA.
E-mail address: cchen@lsuhsc.edu (C. Chen).
[1] Present address: School of Life Sciences and Technology, Tongji University, Shanghai, China.
[2] Present address: Department of Pharmacology, School of Pharmacy, China Pharmaceutical University, Nanjing, China.
[3] Present address: State Key Laboratory of Stem Cell and Reproductive Biology, Institute of Zoology, Chinese Academy of Sciences, Beijing, China.

and that disturbance of synaptic structure and function causes brain disorders [5].

MicroRNAs are small non-coding RNAs that inversely regulate expression, stability, and function of target molecules at the post-transcriptional level by complementary binding to the three-prime untranslated region (3′-UTR) of target mRNAs [6,7]. Dysregulation of miRNAs in the brain has been implicated in neurodegenerative diseases, including AD [8–17]. For examples, it has been shown previously that expression of miRNAs that target β-secretase (BACE1), a key enzyme responsible for synthesizing Aβ, is reduced in the brains of both AD patients and APP transgenic (TG) mice, animal models of AD [18–21]. Reduced expression of these miRNAs may cause increases in expression and function of BACE1, resulting in aberrant production of Aβ in AD. Several miRNAs that regulate synaptic function have been identified previously in normal control animals [22–27]. However, very few studies have been conducted to determine whether expression of miRNAs that target molecules important for regulation of synaptic structure and function is dysregulated in AD [28,29]. Here, we provide evidence for the first time that expression of miR-30b, which targets molecules important for maintaining synaptic integrity, including ephrin type-B receptor 2 (ephB2), sirtuin1 (sirt1), and glutamate receptor subunit 2 (GluA2), is robustly upregulated, while expression of its targets, is significantly downregulated in the hippocampi of both AD patients and 5XFAD APP transgenic (TG) mice. Overexpression of miR-30b in the hippocampus of normal wild-type (WT) mice impairs basal synaptic transmission and long-term potentiation (LTP), learning and memory and reduces the density of dendritic spines and expression of synaptic proteins, including PSD-95 and glutamate receptor subunits, mimicking those seen in TG mice. Conversely, knockdown of endogenous miR-30b by miRNA 'sponging' in TG mice prevents synaptic and cognitive declines and as well as decreases in expression of synaptic proteins and densities of dendritic spines. Our results reveal a previously undefined mechanism that underlies abnormality of synaptic structure and function in AD, suggesting that reversal of dysregulated miR-30b in the brain may prevent or slow synaptic and cognitive declines in AD.

2. Methods

2.1. Animals

C57BL/6J mice (Stock number: 000664) and 5XFAD APP transgenic (TG) mice (Stock number: 006554) were obtained from the Jackson Laboratory, as described previously [30]. TG and age-matched wild-type (WT) littermates were used in the studies as describe previously [20,31].

2.2. Human brain tissues

Human hippocampal tissues used in this study were provided by NIH/Harvard Brain Tissue Resource Center and BioChain Institute Inc. (Newark, CA).

2.3. Cell culture

Mixed neurons and astroglial cells (astroglial cells~5%), NG108–15, and HEK 293/293T cells were cultured as described previously [20,31–35]. The extent of neurons and astroglial cells in culture were estimated by using immunostaining with NeuN, a neuronal marker, glial fibrillary acidic protein (GFAP), an astrocytic marker, and OX-42, a microglial marker, in conjunction with DAPI staining.

2.4. Functional validation

Based on our miRNA microarray analysis [20], we observed that expression of miR-30b was robustly elevated in the hippocampus of TG mice. We used online webs to search computationally predicted targets of miR-30b and identified that miR-30b has computationally predicted binding sites (BS) in the 3′UTR of ephB2 (BS: nt 825–832), sirt1 (BS: nt 72–78), and GluA2 (BS: nt 2461–2468). The sequences incorporating the putative miR-30b binding sites of the 3′UTRs of ephB2, sirt1 and GluA2 were amplified from mouse genomic DNA by PCR and cloned in the dual luciferase reporter vector psiCHECK vector (Promega, Madison, WI). Primers were used for the 3′UTRs of ephB2, sirt1 and GluA2 as followings: EphB2 forward: CTCGAG GGCAGACAGGAGGATAGTTGTT, EphB2 reverse: TGCGGCCGC GGGCGCTGATGTAGTTC; Sirt1 forward: CTCGAG GTTTAGAAGAACCCTTGGAAGATG, Sirt1 reverse: GCGGCCGC AACTAAGGGGACCTATATAGACAGGC; GluA2 forward: CTCGAG GAGT ATGAATAATGTTGATTG, GluA2 reverse: GCGGCCGCCATACACTTTTGGT TTCTCA. The luciferase reporter construct was cotransfected with the miR-30b expression plasmid into HEK 293T cells. The putative miR-30b recognition in the 3′UTR of ephB2, sirt1 and GluA2 was further validated by the luciferase reporter vector expressing mutated BS in the 3′ UTR of ephB2, sirt1 and GluA2. Mutations of the BS sequences were made in the 3′UTR of ephB2, sirt1 and GluA2 recognized by the seed region of miR-30b. The primers of the mutated BS in the 3′UTRs: ephB2 forward: CATACTCTTGCATCTGGGTTTGGACCCAGCGATTCCGTGGACCG GGG, ephB2 reverse: CCCCGGTCCACGGAATCGCTGGGTCCAAACCCAG ATGCAAGAGTATG; Sirt1 forward: TTAGCATGTCAAAAAATGAATGGACC CTTGTGAACTTGAACAAGGAAATC, Sirt1 reverse: GATTTCCTTGTTCAAG TTCACAAGGGTCCATTCATTTTTTGACATGCTAA; GluA2 forward: TTGTCC TTTACTGTACATTTTGGACCCAGTATAGTACCTTATTCTCT, GluA2 reverse: AGAGAATAAGGTACTATACTGGGTCCAAAATGTACAGTAAAGGACAA. All the constructs were verified by sequencing. The reporter activity (light units) was detected using a microplate luminometer.

2.5. Plasmid and lentiviral constructs

The FUGW lentiviral vector, as described previously [20], was used to insert a miR-30b short hairpin RNA driven by a U6 promoter and the GFP reporter gene driven by a ubiquitin promoter. The primers for cloning miR-30b in the lentiviral vector are as followings: forward: 5′ GACGTTCGAATCTAGAGATCCGACGCCGCCATC3′, and reverse: 5′GACG

TTAATTAAAAAAAAAATGTAAACATCCTACACTCAGCTTCTCTTGAAAGCTGA GTGTAGGATGTTTACAAAACAAGGCTTTTCTCCAAGGGA3′. PCR product was then digested and ligated into the BstB1-Pac1 sites in a modified FUGW2.1 construct with U6 promoter. To reduce the endogenous miR-30b level, LV containing a miR-30b sponge (miR-30bs, containing six bulged miR-30b binding sites that are separated by AATT spacers) was cloned by annealing the pair of primers into the NheI-AgeI sites in the LIB01 LV vector (Supplementary Fig. 4). pCMVΔ8.9 and VSVg vectors were used for viral envelope and production in 293T cells and titered by fluorescence-activated cell sorter (FACS) analysis using a flow cytometry as described previously [20,31]. The titer of the LV at least 1.0×10^{10} was used for in vivo injections.

2.6. Stereotaxic injection

Wild-type and APP TG mice at 4 months of age were anesthetized with ketamine/Xylazine (200/10 mg/kg). LV-controls, LV-miR-30b, or LV-miR-30bs (2 μl at 0.2 μl /min/each side) was stereotaxically injected into the hippocampus at the coordinate: AP, −2, ML, ±1.8, and DV, −2, with a 5 μl of Hamilton microsyringe, as described previously [20]. All the assays were carried out 8 weeks after LV injections.

2.7. Reverse transcription and real-time PCR

Total RNA was extracted from hippocampal tissues or cells using the RNeasy Mini Kit and treated with RNase-free DNase as described previously [20]. 1 μg of total RNA was used with 4 μl 5× iscript reaction mix and 1 μl iscript reverse transcriptase. Samples (20 μl) were incubated for 5 min at 25 °C, and then were then heated to 42 °C for 30 min. The reaction was stopped by heating to 85 °C for 5 min. The primers for miR-30b and U5/U6 were obtained from QIAGEN (Valencia, CA). The primers for glyceraldehyde-3-phosphate-dehydrogenase (GAPDH) were selected using Beacon Designer Software (BioRad) and synthesized by IDT (Coralville, IA): forward primer, reverse primer (amplicon size), genebank number: 5′-ACCACAGTCCATGCCATCAC-3′, 5′-ACCTTG CCCACAGCCTTG-3′ (134 bp), M32599. All the PCR products were verified by sequencing. We used the relative CT method to calculate RNAs as the fold increase or decrease, which was determined relative to the control after normalizing to a housekeeping gene using $2^{-\Delta\Delta CT}$, where ΔCT is (gene of interest CT) - (GAPDH CT), and ΔΔCT is (ΔCT treated) - (ΔCT control), as described previously [20,34–36].

2.8. Immunoblot

The immunoblot assay was used to determine expression of ephB2, sirt1, GluA1, GluA2, GluN2B, PSD-95, BACE1, Nicastrin, ADAM-10, Aβ42, and p-NF-κB in hippocampal tissues from WT or TG mice. Hippocampal tissue was extracted and immediately homogenized in RIPA lysis buffer and protease inhibitors, and incubated on ice for 30 min, then centrifuged for 10 min at 10,000 rpm at 4 °C. Supernatants were fractionated on 4–15% SDS-PAGE gels (Bio-Rad) and transferred onto PVDF membranes (Bio-Rad). A special 16.5% Criterion™ Tris-Tricine Gelforgel (Bio-Rad) was used for detecting Aβ42 immunoreactivity. The antibodies used to detect the expression of following proteins: Anti-ephB2 (1:200, Abcam, Cat# AB5418), anti-sirt1 (1:1000, EMD Millipore, Cat# 09–844), anti-GluA1 (1:1000, EMD Millipore, Cat# AB1504), anti-GluA2 (1:1000, EMD Millipore, Cat# MAB397), anti-GluN2B (1:1000, Abcam, Cat# ab73001), anti-PSD-95 (1,1000, Abcam, Cat# ab18258), anti-Aβ42 (1:1000, Invitrogen), anti-BACE1 (1:1000, Covance), anti-p-NF-kB (1:1000, Cell Signaling). We incubated the membrane with specific antibodies at 4 °C overnight, washed and incubated the blot with a secondary antibody (goat anti-rabbit 1:2000, Cell Signaling, Danvers, MA) at room temperature for 1 h. Proteins were detected by enhanced chemiluminescence (Amersham Biosciences, UK). The densities of specific bands were quantified by densitometry using FUJIFILM Multi Gauge software (version 3.0). Signal intensities were normalized to

mouse anti β-actin (1:4000, Sigma), as described previously [20,31,34,36,37].

2.9. Immunocytochemistry and immunohistochemistry

Immunostaining was used to detect expression of GFP and formation of total Aβ in coronal sectioned brain slices and detect expression of GFP, ephB2, sirt1, GluA2 and PSD-95 in cultured neurons. WT or TG mice that received LV-Con, LV-miR-30b or LV-miR-30bs for 8 weeks were anesthetized with ketamine/Xylazine (200/10 mg/kg) and subsequently transcardially perfused with PBS followed by 4% paraformaldehyde in phosphate buffer. Cryostat sectioning was made on an Leica freezing Vibratome at 40 μm and series sections (10 to 12 slices) were collected in 0.1 M phosphate buffer. Free floating sections or cultured neurons were immunostained using antibodies specific for total Aβ (4G8, 1:2000, Millipore). The fluorescent signals were detected using a Zeiss deconvolution microscope with SlideBook 5.5 software and the imaging data were analyzed and quantified using SlideBook 5.5 as described previously [20,31,35–37].

2.10. Golgi–Cox staining

Golgi–Cox staining was used to detect dendritic spines of hippocampal neurons as we described previously with modification [38]. 6-month old WT or TG mice injected with LV-miR-30b or LV-30bs were anesthetized with ketamine/Xylazine (200/10 mg/kg) and subsequently transcardially perfused with ice-cooled saline for 5 min. The brain was dissected out and processed with Golgi-Cox Impregnation & Staining System according to the manufacture's instruction (supperGolgi Kit, Bioenno Tech, LLC, Cat# 003010). After impregnation, sections (100 to 200 μm) were obtained using a vibratome and the sections were mounted on gelatin-coated glass slides, and stained [38]. Images were taken by using a Zeiss Imager II deconvolution microscope with SlideBook 5.5 software. For quantification of spines, images were acquired as a series of z-stack at 0.1-μm step to create sequential images enabling spine counting, and spine morphology measurements on 3D images using a 100 X oil objective. NeuronStudio (Version 0.9.92; http://research.mssm.edu/cnic/tools-ns.html, CNIC, Mount Sinai School of Medicine) was used to reconstruct and analyze dendritic spines as described previously [31,37].

2.11. FISH analysis

miRCURY LNA™ Detection probes for miR-30b and scramble miR-30b (Exiqon, Woburn, MA) were used for fluorescence in situ hybridization (FISH) analysis of miR-30b on 10 μm frozen sections of mouse and human brains and in cultured hippocampal neurons, according to the manufacture's instruction as well as a previously described protocol [39].

2.12. ChIP analysis

Chromatin Immunoprecipitation (ChIP) analysis was carried out as described previously [20,31] to detect the binding of NF-κBp65 in the promoter of the miR-30b gene. The primers for CHIP: forward primer: 5′- TGTTTGCTTCCTCCTCCTGT-3′ and reverse primer: 5′- CCACAAGGG CATACAGAACC-3′ for the binding site 1, and 5′- CCACATAATTCACCCA TTTCC-3′, and 5′-TG TGTTTGAAAACCGCTAGA-3′ for the binding site 2.

2.13. Hippocampal slice preparation

Hippocampal slices were prepared as described previously [20,31,36,37,40]. Briefly, after decapitation, brains were rapidly removed and placed in ice cold oxygenated (95% O_2, 5% CO_2) low-Ca^{2+}/high-Mg^{2+} slicing solution composed of (in mM): 2.5 KCl, 7.0 $MgCl_2$, 28.0 $NaHCO_3$, 1.25 NaH_2PO_4, 0.5 $CaCl_2$, 7.0 glucose, 3.0 pyruvic acid,

1.0 ascorbic acid, and 234 sucrose. Slices were cut at a thickness of 350 µm and transferred to a holding chamber in an incubator containing oxygenated artificial cerebrospinal fluid (ACSF) composed of (in mM): 125.0 NaCl, 2.5 KCl, 1.0 MgCl₂, 25.0 NaHCO₃, 1.25 NaH₂PO₄, 2.0 CaCl₂, 25.0 glucose, 3 pyruvic acid, and 1 ascorbic acid at 36 °C for 0.5 to 1 h, and then maintained in an incubator containing oxygenated ACSF at room temperature (~22–24 °C) for >1.5 h before recordings. Slices were then transferred to a recording chamber continuously perfused with 95% O_2, 5% CO_2-saturated ACSF at ~32–34 °C.

2.14. Electrophysiological recordings

Extracellular field excitatory postsynaptic potentials (fEPSPs) were recorded in response to stimuli at perforant path synapses in the dentate gyrus of the hippocampus at a frequency of 0.05 Hz using an Axoclamp-2B patch-clamp amplifier (Molecular Devices, Sunnyvale, CA), as described previously [20,36]. Long-term potentiation (LTP) was induced by a high-frequency stimulation (HFS) consisting of two trains of 100 Hz stimulation (1 s duration and a 20 s inter-train interval). The input-output function was tested before recording of LTP, and the baseline stimulation strength was set to provide fEPSP with an amplitude of ~30% from the sub-threshold maximum derived from the input-output function. A paired-pulse protocol with various inter-pulse intervals was used to determine short-term synaptic plasticity.

Whole-cell patch-clamp recordings were made using an Axopatch-200B patch-clamp amplifier (Molecular Devices, Sunnyvale, CA) under voltage clamp as described previously [37,41]. Pipettes (2–4 MΩ) were pulled from borosilicate glass with a micropipette puller (Sutter Instrument, Novato, CA). The internal pipette solution contained (in mM): 90.0 CsCH₃SO₃, 40.0 CsCl, 10.0 HEPES, 5.0 CaCl₂, 4.0 Mg₂ATP, 0.3 Na₂GTP, and 5.0 QX-314, or 130 KCH₃SO₄, 10 KCl, 4 NaCl 10 HEPES, 0.1 EGTA, 4 Mg₂ATP, 0.3 Na₂GTP, and 5 QX-314. The membrane potential was held at −70 mV. Evoked excitatory postsynaptic currents (EPSCs) in dentate granule neurons were recorded in response to stimuli of perforant path synapses (PP) at a frequency of 0.05 Hz via bipolar tungsten electrodes. Miniature spontaneous EPSCs were recorded in cultured hippocampal neurons treated with LV-miR-30b, LV-miR-30bs or LV-control. The amplitude, frequency, and kinetics of mEPSCs were analyzed using the MiniAnalysis program. SR95531 (gabazine, 1 µM) was used to block GABAergic synaptic transmission during recordings.

Outside-out patch recordings were made using an Axopatch-200B patch-clamp amplifier as described previously [41,42]. Outside-out patches were excised from cultured mouse hippocampal neurons treated with LV-miR-30b, LV-miR-30bs or LV-control, and the membrane potential was held at −70 mV. Glutamate-induced currents were induced through a Burleigh fast solution switching system to deliver control and glutamate (1 mM) solutions via a theta glass tubing [41].

2.15. Behavioral test

The classic Morris water maze test was used to assess spatial learning and memory as described previously [20,31,36,37]. A circle water tank (diameter 120 cm and 75 cm in high) was filled with water, which was made opaque with non-toxic white paint. A round platform (diameter 15 cm) was hidden 1 cm beneath the surface of the water at the center of a given quadrant of the water tank. Acquisition training was carried out continuous 7 days (7 sessions) and each session consisted of 4 trials. For each trial, the mouse was released from the wall of the tank and allowed to search, find, and stand on the platform for 10 s within the 60-sec trial period. For each training session, the starting quadrant and sequence of the four quadrants from where the mouse was released into the water tank were randomly chosen so that it was different among the separate sessions for each animal. The probe test was performed 1 day after the completion of the 7-day's training. During the probe test, the platform was removed from the

pool, and the task performance was recorded for 60 s. The mice in the water pool were recorded by a video-camera and the task performances, including swimming paths, speed, and time spent in each quadrant were recorded by using an EthoVision video tracking system (Noldus).

The novel object recognition and exploration test was performed as described previously [43]. Briefly, animals were first allowed to acclimate to the testing environment (habituation). The test included two stages: training and testing. In the first stage of the test, the animal was confronted with two identical objects, placed in an open field, and in the second stage, the animal was exposed to two dissimilar objects placed in the same open field: one familiar object, used in the first phase, and the other novel object. Exploration of an object was defined as time spent with the head oriented towards and within two cm of the object. The time spent exploring each of the objects in stage two was detected using the video tracking system.

2.16. Statistics

All values are expressed as mean ± S.E.M. Student's *t*-test and analysis of variance (ANOVA) with post-hoc tests were used for statistical comparison when appropriate. Differences were considered significant when $P < 0.05$.

2.17. Ethics statement

All experiments using animal were conducted in compliance with the US Department of Health and Human Services Guide for the Care and Use of Laboratory Animals and the care and use of the animals reported in this study were approved by the Institutional Animal Care and Use Committee of Louisiana State University Health Sciences Center. The use of postmortem human tissues samples was in accordance with and approved by the institutional review board at the LSU Health Sciences Center.

2.18. Data availability

Data supporting the findings of this manuscript are available from the corresponding authors upon request.

3. Results

3.1. Expression of miR-30b is upregulated in the brains of both AD patients and TG mice

Our previous miRNA microarray screening analysis showed that a significant number of miRNAs was upregulated or downregulated in 5XFAD APP transgenic (TG) mice compared with their wild-type (WT) littermate controls [20]. In particular, we identified that expression of miR-30b, which has computationally predicted binding sites in the 3′-UTRs of ephB2, sirt1, and GluA2 (Supplementary Fig. 1), is upregulated in the brains of TG mice. The upregulation was confirmed in the hippocampus of 6-month old TG mice (Fig. 1a). To determine whether expression of miR-30b is also upregulated in the brains of AD patients, we assessed expression of miR-30b in postmortem hippocampal tissues of patients with AD and of normal subjects. As shown in Fig. 1A, expression of miR-30b is also robustly elevated in the brains of AD patients. The data from fluorescent in situ hybridization (FISH) analysis show that miR-30b is primarily expressed in neurons of the brain (Supplementary Fig. 2). EphB2 and sirt1 have been shown to play important roles in regulation of synaptogenesis, axon guidance, dendritic spine formation and synaptic maturation, expression and function of AMPA and NMDA glutamate receptors, long-term synaptic plasticity, and memory formation [44–50], while GluA2 is an important subunit of the AMPA glutamate receptor. Therefore, upregulated expression of miR-30b in the brains of both AD patients and TG mice suggests that

dysregulated miR-30b may contribute to synaptic dysfunction in AD. In addition, we observed that expression of miR-30b does not display gender-specific in both human normal subjects and AD patients as well as in normal WT mice or in TG mice (Supplementary Fig. 3a). Also, there is no difference in expression of miR-30b in female mice during the estrous cycle (Supplementary Fig. 3b).

3.2. Functional validation of the predicted binding sites of miR-30b in the 3′ UTRs ephB2, sirt1, and GluA2

To validate the putative binding sites (BS) of miR-30b, we used luciferase reporter constructs inserted with the 3′-UTR of ephB2, sirt1 or GluA2. As shown in Fig. 1b, co-transfection of the reporter vector with the pEGP vector expressing miR-30b in 293 cells resulted in inhibition of the reporter activities compared with the controls. To further validate the interaction of miR-30b with these targets, we mutated the BS sequences in the 3′-UTR of the target molecules recognized by the seed region of miR-30b and observed that co-transfection of the BS-mutated reporter vectors with the vector expressing miR-30b led to loss of inhibition of the reporter activities compared with the WT control (Fig. 1b). These results indicate that miR-30b functionally binds to the 3′-UTRs of ephB2, sirt1, and GluA2.

3.3. miR-30b represses its targets ephB2, sirt1, and GluA2

To determine the ability of miR-30b to repress its target molecules, we generated lentiviral vector (LV) expressing miR-30b (LV-miR-30b) as described previously [20]. As shown in Fig. 1c, a treatment with LV-miR-30b in cultured hippocampal neurons resulted in a significant decrease in expression of miR-30b targets, including ephB2, sirt1 or GluA2 by immunoblot analysis. The repression of these targets by miR-30b was further confirmed by immunocytochemistry (Fig. 1d), suggesting that an increased expression of miR-30b correlates with a decreased expression of ephB2, sirt1 or GluA2.

To determine whether changes in expression of miR-30b alter synaptic structure and function, we designed and generated LV-expressing miR-30b sponge (LV-miR-30bs) to render endogenous miR-30b loss-of-function (Supplementary Fig. 4), as described previously [20,23,51]. Hippocampal neurons in culture treated with LV-miR-30bs displayed a reduced expression of endogenous miR-30b by FISH and qPCR analyses (Fig. 1e&f), suggesting that LV-miR-30bs sequesters endogenous miR-30b in vitro.

3.4. Changes in miR-30b levels alter synaptic function

Since miR-30b targets the molecular important for maintaining synaptic integrity, we asked whether changes in expression levels of miR-30b alter synaptic function both in vitro and in vivo. To determine the effects of miR-30b on synaptic activity, we recorded spontaneous miniature excitatory postsynaptic currents (mEPSCs) in primary cultured hippocampal neurons treated with LV-miR-30b, LV-miR-30bs, or LV-control. As shown in Fig. 1g, overexpression of miR-30b reduced the amplitude of mEPSCs, while a decrease in miR-30b expression by 'sponging' increased the amplitude of mEPSCs. suggesting that changes in the amplitude of mEPSCs by miR-30b overexpression or sequestration are likely associated with alterations in expression of postsynaptic glutamate receptors. This prediction was further confirmed by recordings of direct application of glutamate-induced currents in cell-free outside-out patches excised from cultured hippocampal neurons treated with LV-miR-30b, LV-miR-30bs, or LV-control. As shown in Fig. 1h, overexpression of miR-30b reduced the amplitude of glutamate-induced currents, while the knockdown enhanced the currents. These results from in vitro experiments suggest that expression of glutamate receptor subunits is regulated by miR-30b through repression of its targets ephB2, sirt1 and GluA2. To confirm this speculation, LV-miR-30b, LV-miR-30bs or LV-scramble control were stereotaxically injected into the hippocampus in 2-month-old normal C57BL/6 mice (Fig. 1i) and the assessment was carried out 2 months after injections. As shown in Fig. 1J&K, overexpression of miR-30b decreased the amplitude of excitatory postsynaptic currents (EPSCs) and input-output function at hippocampal synapses, while sequestration of endogenous miR-30b by miR-30b 'sponge' enhanced them, supporting the findings from in vitro studies.

### 3.5. miR-30b regulates expression of its targets in AD

As shown in Fig. 1A, expression of miR-30b is robustly elevated in the brains of both AD patients and TG mice. Since miRNAs inversely regulate its target mRNAs, we predicted that upregulated expression of miR-30b represses its targets in AD. Indeed, we observed that expression of ephB2, sirt1 or GluA2 was significantly reduced in the hippocampal tissues of both AD patients and TG mice (Fig. 2a). If reduced expression of ephB2, sirt1 or GluA2 in the brains of both AD patients and TG mice is due to elevated expression of miR-30b, then, overexpression of miR-30b would repress its targets in normal WT animals, while knockdown of endogenous miR-30b would rescue reduced expression of the targets in TG mice. To test this hypothesis, LV-miR-30b, LV-miR-30bs or LV-scramble control was stereotaxically injected into the hippocampus of 4-month-old WT or TG mice and the analysis was performed 2 months after LV injections (6-month-old). As shown in Fig. 2b, the level of hippocampal miR-30b was elevated in WT mice injected with LV-miR-30b, while upregulated endogenous miR-30b in TG mice was suppressed by LV-miR-30bs. As expected, expression of miR-30b targets, including ephB2, sirt1 or GluA2, in the hippocampus was significantly reduced in WT mice injected with LV-miR-30b, while the reduced expression of the targets was returned to normal control levels in TG mice injected with LV-miR-30bs (Fig. 2c), further supporting the idea that ephB2, sirt1 or GluA2 are regulated by miR-30b. However, we noticed that overexpression or knockdown of miR-30b in WT or TG mice did not alter production of Aβ and expression of the enzymes synthesizing Aβ. As shown in Fig. 2d&e, no Aβ42 or Aβ plaques were formed and no changes in expression of the enzymes responsible for the Aβ synthesis were observed in WT mice injected with LV-miR-30b. As demonstrated previously, 5XFAD mice display elevated expression of BACE1 and γ-secretase (e.g., Nicastrin, a component of γ-secretase complex) as well as accumulated Aβ plaques in the brain at age of 6 month [20,30,37]. We observed that knockdown of miR-30b by miR-30b 'sponging' did not reduce Aβ42, Aβ plaques, BACE1 or Nicastrin (Fig. 2d&e), suggesting changes in the levels of miR-30b do not affect Aβ processing.

3.6. Overexpression of miR-30b impairs synaptic transmission and plasticity in WT mice and knockdown of miR-30b prevents deterioration in synaptic function in TG mice

If impaired synaptic function in AD results from the elevated expression of miR-30b, then overexpression of miR-30b should impair synaptic function in normal WT mice, mimicking those seen in TG mice. Conversely, sequestration of endogenous miR-30b should alleviate synaptic deficits in TG mice. To test this prediction, we assessed hippocampal basal synaptic transmission in terms of input-output function and synaptic plasticity in terms of long-term potentiation (LTP) in WT mice injected with LV-miR-30b or TG mice injected with LV-miR-30bs. As shown in Fig. 3a&b, overexpression of miR-30b in WT mice led to impairments in input-output function and LTP, which mimics those seen in TG mice [20,37]. In contrast, impaired basal synaptic transmission and long-term synaptic plasticity in TG mice were rescued by knockdown of endogenous miR-30b, suggesting that upregulated expression of miR-30b causes synaptic dysfunction.
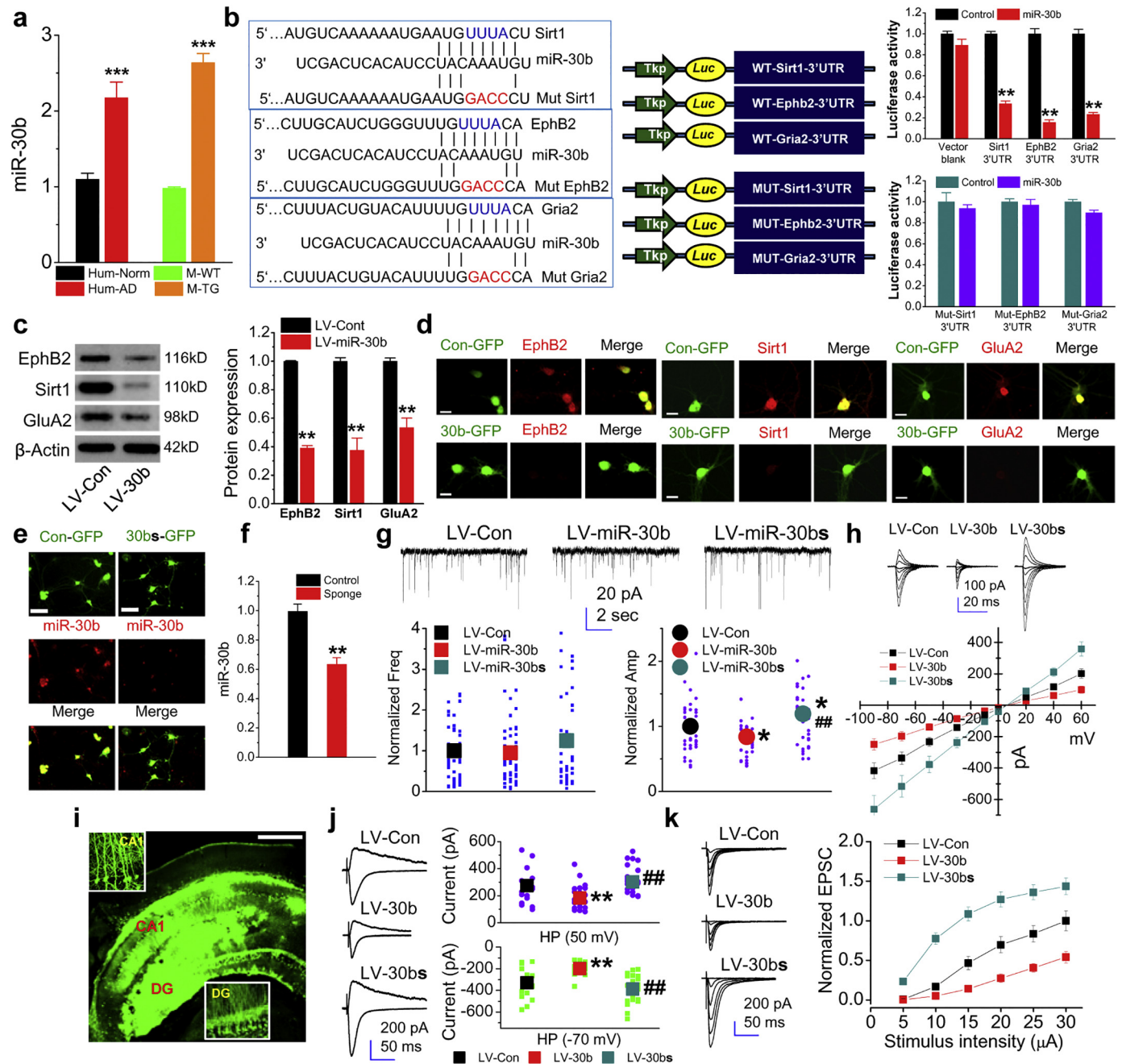
Fig. 1. Non-coding small RNA miR-30b that targets the molecules important for synapses is upregulated in Alzheimer's disease (AD). (a) Expression of miR-30b is upregulated in the hippocampus of both AD patients and 5XFAD transgenic (TG) mice (Animals: ***P < 0.001, Student's t-test, n = 22/group; Humans: ***P < 0.001, n = 14/normal and n = 15/AD). The postmortem human hippocampal tissues were from normal controls at ages of 80.1 ± 3.3 years and from AD patients at ages of 76.3 ± 3.1 years with the mean post-mortem interval (PMI) 7.4 ± 1.2 h and 6.6 ± 0.9 h, respectively. (b) Binding sites of miR-30b in the 3′UTRs of ephB2, sirt1 and GluA2 recognized by the seed region of miR-30b. The luciferase reporter activity in 293 cells transfected with psiCHECK vector of wild-type (normal) and mutated binding sites in the 3′UTR of ephB2, sirt1, and GluA2 recognized by the seed region of miR-30b in the absence and presence of miR-30b. (**P < 0.01, n = 3/group). (c) Immunoblot analysis of ephB2, sirt1, and GluA2 expression in cultured hippocampal neurons transfected with LV-miR-30b or LV-control (**P < 0.0001, n = 7/group). (d) Immunostaining analysis of ephB2, sirt1, and GluA2 expression in cultured hippocampal neurons treated with LV-miR-30b or LV-control. Scale bar: 20 μm. (e) Endogenous miR-30b is sequestered by miR-30b 'sponging' (miR-30bs). FISH analysis was performed to detect expression of miR-30b in cultured hippocampal neurons treated with LV-scramble control or LV-miR-30bs. Scale bar: 30 μm. (f) qPCR analysis of knockdown of miR-30b by miR-30bs. **P < 0.01, n = 3/group with duplicates. (g) Spontaneous miniature excitatory postsynaptic currents (mEPSCs) recorded in cultured hippocampal neurons treated with LV-miR-30b, -LV-miR-30bs ('sponge') or -LV-control (*P < 0.05 compared with LV-control, ##P < 0.01 compared with LV-miR-30b, ANOVA with Bonferroni post hoc-test, n = 61 recordings in LV-control group, 58 in LV-miR-30b, and 51 in LV-miR-30bs, respectively). (h) Glutamate-induced currents in cell-free outside-out patches excised from cultured hippocampal neurons treated with LV-control, miR-30b, or miR-30bs (n = 25: LV-control group, n = 30: LV-miR-30b, and n = 28: LV-miR-30bs, respectively). Glutamate-induced currents were induced through a Burleigh fast solution switching system to deliver control and glutamate solutions via a theta glass tubing. (i) Stereotaxic injection of LV into the hippocampus and enlarged GFP expression in dentate granule neurons and CA1 pyramidal neurons. Scale bar: 200 μm. (j) EPSCs recorded at holding potential of +50 and − 70 mV in hippocampal slices from normal C57BL/6 mice injected with LV-control, −miR-30b, or –miR-30bs (** < 0.01, compared with LV-control, ##P < 0.01 compared with LV-miR-30b, ANOVA with Bonferroni post hoc-test, n = 18: LV-control group, n = 19: LV-miR-30b, and n = 22: LV-miR-30bs, respectively). (k) Input-output function of EPSCs at hippocampal synapses (n = 23: LV-control group, n = 25: LV-miR-30b, and n = 25: LV-miR-30bs, respectively).
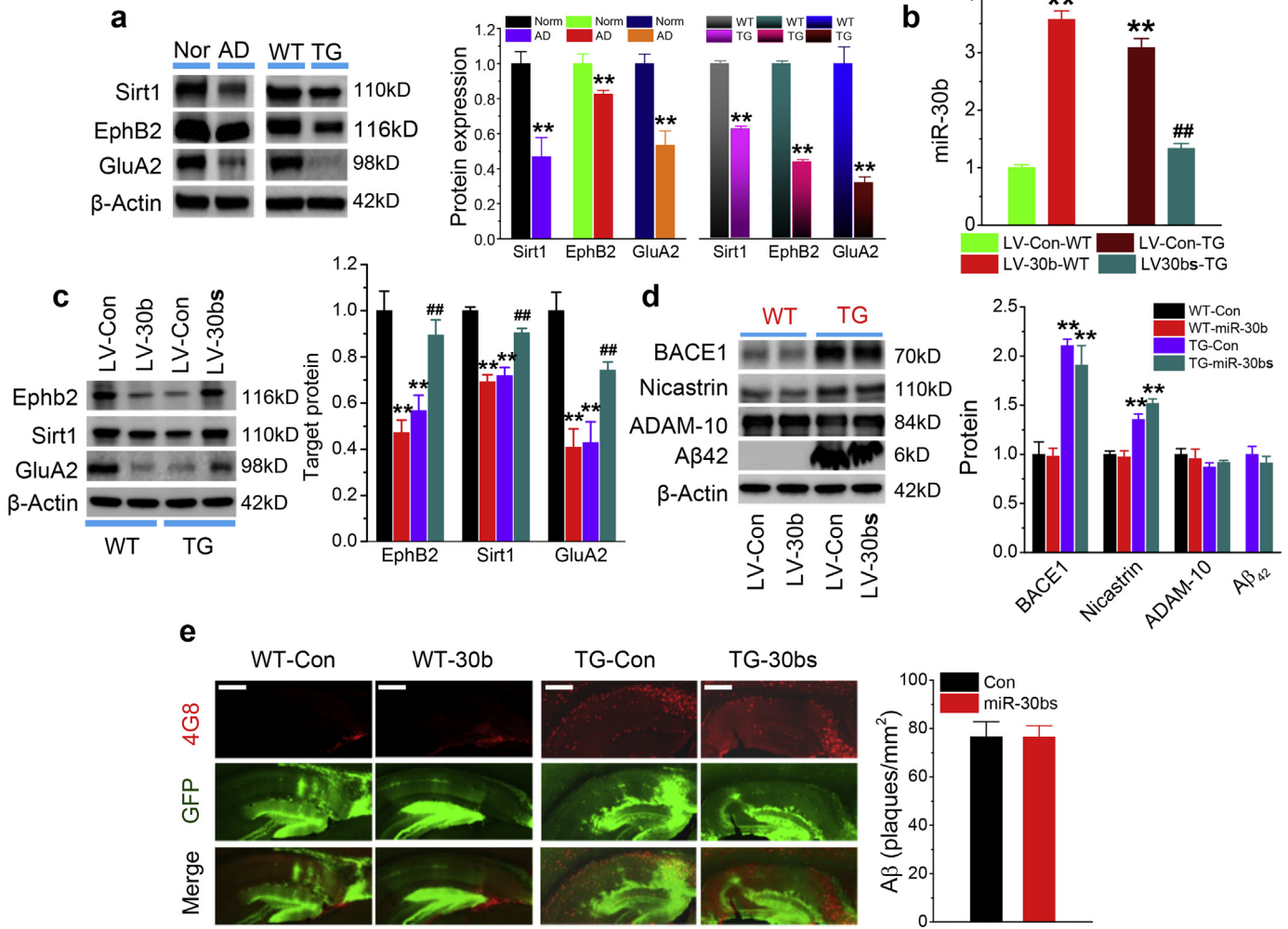
Fig. 2. miR-30b regulates ephB2, sirt1 and GluA2 in the hippocampus. (a) Expression of ephB2, sirt1, and GluA2 is significantly reduced in the hippocampi of both AD patients and TG mice (Humans: **P < 0.01, Student's t-test, n = 4/group; Animals: **P < 0.01, n = 3/group). (b) Changes in expression levels of hippocampal miR-30b by injections of LV-miR-30b in WT mice or LV-miR-30bs in TG mice. LV-control, LV-miR-30b or miR-30bs were stereotaxically injected into the hippocampus of WT or TG mice. qPCR analysis of hippocampal miR-30b expression was conducted 8 weeks after injections. Injection of LV-miR-30b raises hippocampal expression levels of miR-30b in WT mice, while injection of LV-miR-30bs results in a reduction of endogenous hippocampal miR-30b in TG mice. **P < 0.01 compared with WT LV-control and ##P < 0.01 compared with TG LV-control (n = 6/group). (c) Overexpression of miR-30b in the hippocampus represses its targets ephB2, sirt1, and GluA2 in WT mice, while knockdown of miR-30b restores reduced targets in TG mice (ANOVA with Fisher's PLSD test, **P < 0.01 compared with WT-LV-control, ##P < 0.01 compared with TG-LV-control, n = 3/group). (d) Knockdown of endogenous miR-30b does not alter hippocampal production of Aβ42 and the enzymes responsible for synthesis of Aβ. Immunoblot analysis of Aβ42 and and expression of α (ADAM-10), β (BACE1)- and γ (Nicastrin)-secretases in 6-month-old WT or TG mice that received LV-miR-30b or LV-miR-30bs. **P < 0.01 compared with WT LV-control (n = 3 mice/group). (e) Knockdown of endogenous miR-30b by miR-30b sponge does not alter Aβ formation. Immunostaining analysis of total Aβ (all forms) detected by anti-4G8 antibody in the hippocampus of 6-month-old WT mice that received LV-control or LV-miR-30b at 4 months of age or in 6-month-old TG mice that received LV-control or LV-miR-30bs at 4 months of age (n = 5 mice/group).
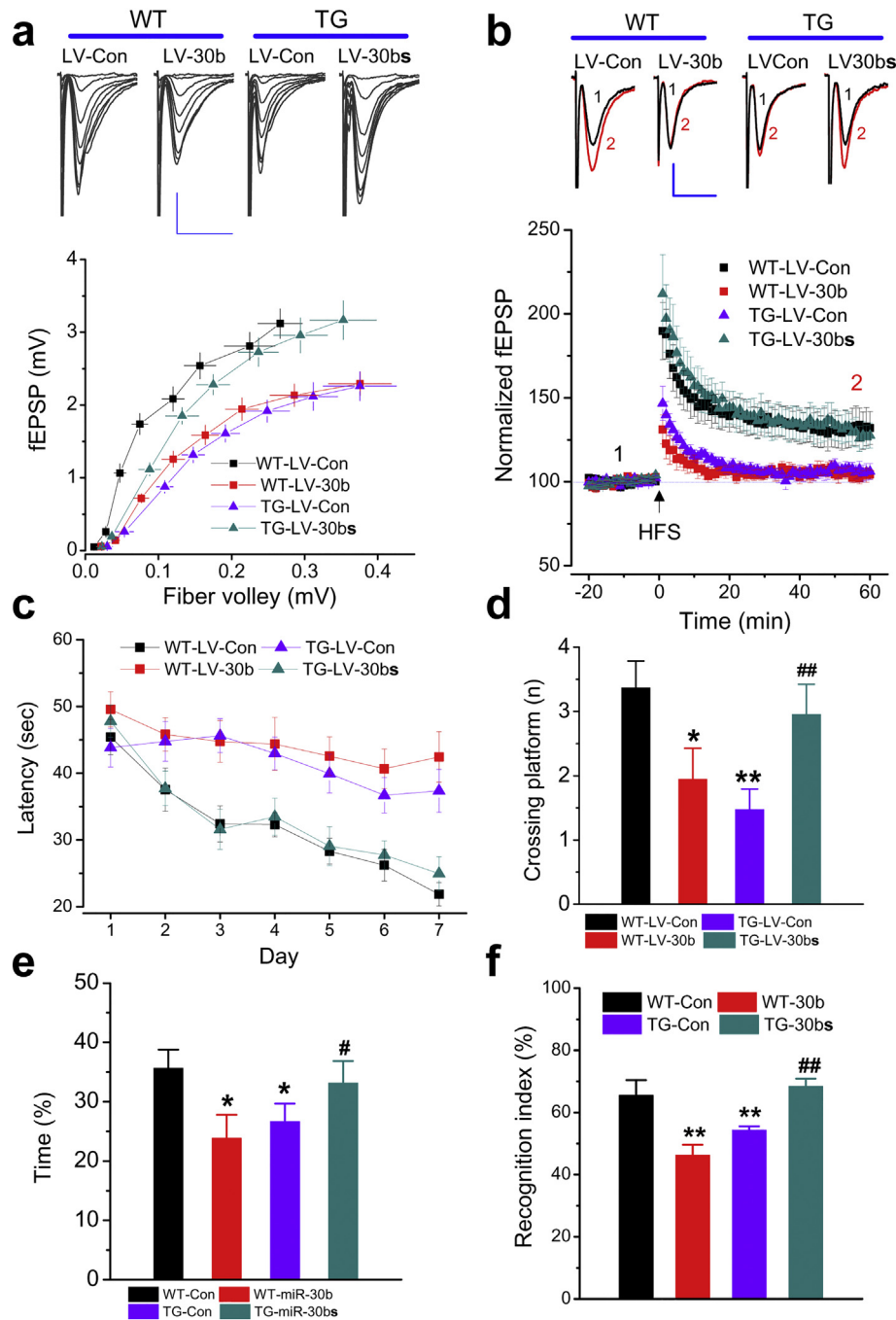
3.7. Overexpression of miR-30b impairs spatial learning and memory in WT mice and knockdown of it prevents cognitive decline in TG mice

We next assessed behavioral performance using the classic Morris water maze and new objective recognition tests in WT mice-treated with LV-miR-30b or in TG mice-treated with LV-miR30bs. As shown in Fig. 3c–e, WT mice injected with LV-miR-30b showed impaired spatial learning and memory retention by displaying prolonged searching time to find the hidden platform during learning acquisition sessions and reduced number of platform crossing and the amount of time spent in the target quadrant during the probe trials, similar to those seen in TG mice in the water maze test. In contrast, TG mice injected with LV-miR-30bs showed improved spatial learning and memory when compared with TG mice injected with LV-control. The impairment in memory retention by increased expression of miR-30b was further confirmed by the new objective recognition test. As shown in Fig. 3f, recognition index was significantly reduced in WT treated with LV-miR-30b and TG mice treated with LV-control. However, the

recognition index in TG mice treated LV-miR-30bs was returned to WT. These results suggest that upregulated miR-30b causes synaptic malfunction, which, in turn, impairs cognitive function in AD.

3.8. miR-30b regulates morphology of dendritic spines and expression of synaptic proteins

It is well established that synaptic function is closely associated with the integrity of synaptic structure. To this end, we asked the question as to whether miR-30b-altered synaptic plasticity and cognitive function are associated with changes in morphology of dendritic spines, where synapses are located, and in expression of synaptic proteins, including PSD-95 and other glutamate receptor subunits. As shown in Fig. 4a, the density of dendritic spines in hippocampal neurons, including granule neurons in the dentate gyrus area and pyramidal neurons in the CA1 region, was significantly reduced in WT mice injected with LV-miR-30b, similar to those in TG mice [37]. In contrast, the reduced density of spines was returned to the WT control levels in TG mice-treated with

Fig. 3. Over-expression of miR-30b impairs synaptic and cognitive function in WT mice and knockdown of miR-30b prevents synaptic and cognitive declines in TG mice. (a) Input-output function recorded at hippocampal perforant synapses (n = 7 animals/WT-LV-Con, n = 6 animals/WT-LV-30b, n = 6 animals/TG-LV-Con, and n = 6 animals/TG-LV-30bs). LV-control, LV-miR-30b, or LV-miR-30bs were stereotaxically injected into the hippocampus in WT or TG mice at 4 months of age. Synaptic and cognitive functions were assessed 2 months after LV injections. (b) Long-term potentiation (LTP) at perforant synapses (n = 6 animals/WT-LV-Con, n = 8 animals/WT-LV-30b, n = 8 animals/TG-LV-Con, and n = 6 animals/TG-LV-30bs). (c) Learning acquisition in the Morris water maze test (ANOVA with repeated measures, P < 0.001, n = 19 animals/group). (d) Crossing the platform in the probe test (ANOVA with Bonferroni post hoc-test, *P < 0.05, **P < 0.01 compared with WT-LV-Con, ##P < 0.001 compared with TG-LV-Con, n = 19/group). (e) The percentage of time spent in the target quadrant during the probe trial. (ANOVA with Bonferroni post hoc-test, *P < 0.05 compared with WT-LV-Con, #P < 0.001 compared with TG-LV-Con, n = 19/group). (f) Novel object recognition test (ANOVA with Bonferroni post hoc-test. **P < 0.01 compared with WT-LV-Con, ##P < 0.01 compared with TG-LV-Con, n = 10/group).

LV-miR-30bs (Fig. 4a). Moreover, hippocampal expression of PSD-95, GluA1, and GluN2B, which are critically important for synaptic transmission and plasticity, was reduced in WT mice-injected with LV-miR-30b, while the reduced expression of these molecules was restored in TG mice-injected with LV-miR-30bs (Fig. 4b). We also noticed that no significant changes in expression of GluN1 and synaptophysin in WT mice treated with LV-miR-30b and in TG mice treated with LV-miR-30bs when compared with their control LV injections. In addition, while expression of GluN2A was not changed in WT mice

overexpressed with miR-30b, expression of GluN2A was significantly reduced in TG mice injected with LV-control or LV-miR30bs, suggesting that expression of GluN2A is not regulated miR-30b (Fig. 4b).

3.9. Expression of miR-30b is upregulated by proinflammatory factors via NF-κB signaling

Finally, we asked the question of why miR-30b is elevated and what causes its changes in AD. Neuroinflammation has long been believed to

contribute to the pathogenesis and neuropathology of AD [52–54]. Nevertheless, a gap in our knowledge is how neuroinflammation triggers synaptic dysfunction in AD. We observed that expression of miR-30b was increased with age in TG mice, but not in WT mice (Fig. 5a). The changes in expression seems to correlate with neuroinflammatory status and gliosis in 5XFAD TG mice [30], suggesting that there is a correlation between neuroinflammation/amyloid burden and miR-30b expression in TG mice. Thus, we hypothesized that upregulation of miR-30 in AD is triggered by neuroinflammatory responses. Indeed, as shown in

Fig. 5b, proinflammatory cytokines and Aβ42, which is also an inflammagen, promoted expression of miR-30b, but the increase was blocked by inhibition of nuclear transcription factor NF-κB signaling pathway. In addition, we detected that phosphorylated NF-κB was significantly elevated in the hippocampus of both AD patients and TG mice (Fig. 5c). These results suggest an involvement of NF-κB signaling in regulation of miR-30b expression. To test this prediction, we performed a chromatin immunoprecipitation (ChIP) analysis and found that the NF-κB p65 subunit displayed the binding activity in the
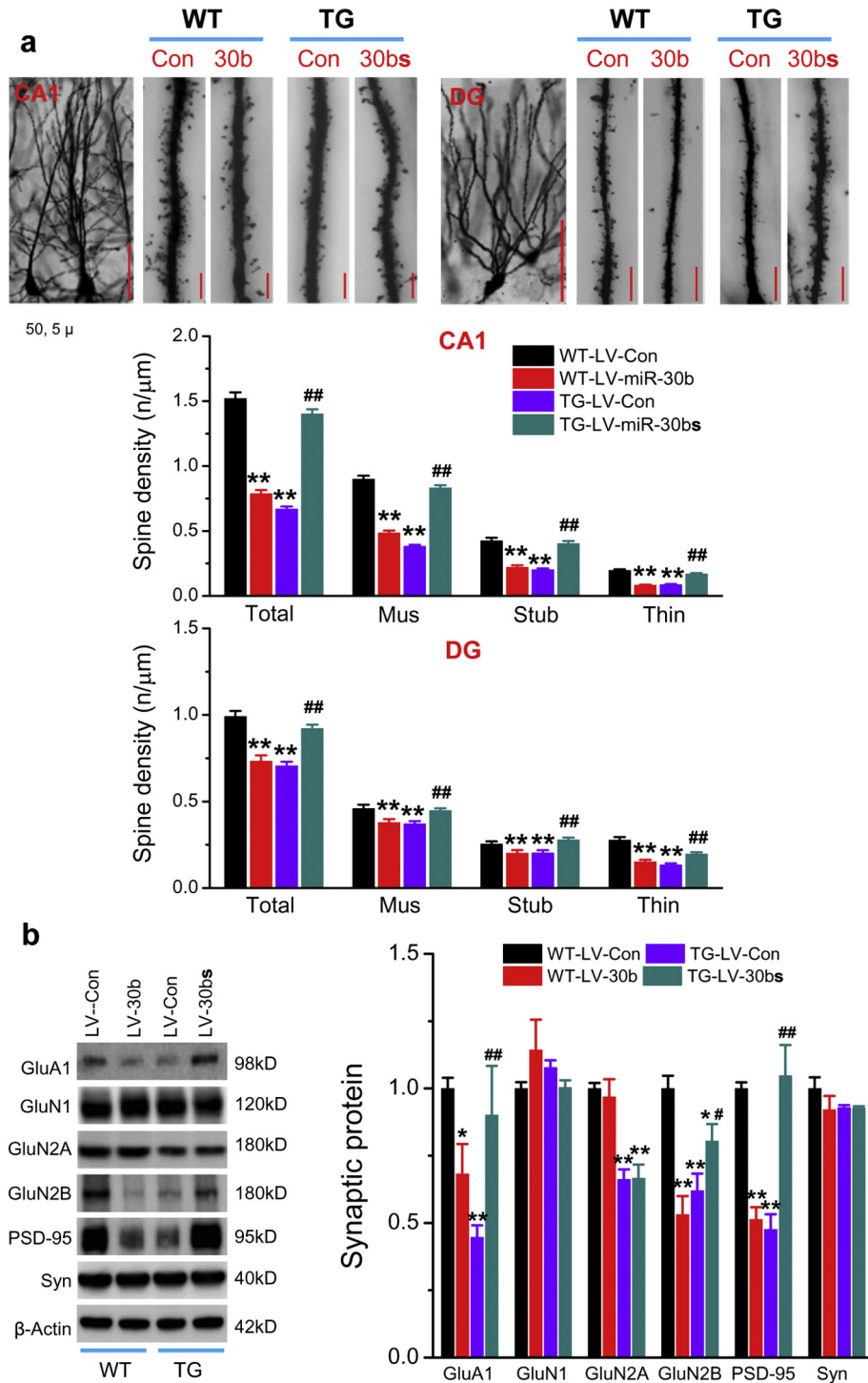
Fig. 4. miR-30b regulates the integrity of synaptic structure. (a) Golgi staining of dendritic spines in hippocampal CA1 pyramidal neurons and dentate granule neurons from WT or TG mice injected with LV-30b, LV-30bs or LV-Con for 8 weeks (ANOVA with Bonferroni post hoc-test, **P < 0.01 compared with WT-LV-Con, ##P < 0.01 compared with TG-LV-Con, n = 6 animals/group). Scale bars: 50 and 5 μm. (b) hippocampal expression of glutamate receptor subunits and PSD-95 in WT or TG mice injected with LV-Con, LV-30b or LV-30bs (ANOVA with Fisher's PLSD test, *P < 0.05, **P < 0.01 compared with WT-LV-Con; #P < 0.05, ##P < 0.01 compared with TG-LV-Con n = 3–6/group).

promoters of the miR-30b gene (Fig. 5d), suggesting NF-κB regulates transcription and expression of miR-30b. This is further supported by evidence that silencing the NF-κB p65 subunit blocked cytokine-induced upregulation of miR-30b (Fig. 5e). These results provide evidence showing that expression of miR-30b in AD is upregulated through neuroinflammation-triggered enhancement of the NF-κB transcriptional activity (Fig. 6).

4. Discussion

AD is a devastating neurodegenerative disease characterized by accumulation and deposition of Aβ plaques and neurofibrillary tangles, neuroinflammation, synaptic dysfunction/loss of synapses, progressive deterioration in cognitive function and loss of memory in association with widespread degenerated neurons/neuronal death. While the etiology of AD is multifactorial and complex, it is widely accepted that synaptic dysfunction and/or loss of synapses are the best pathological correlate of cognitive decline in AD [1–5,55]. However, the mechanisms underlying synaptic failure in AD are largely unknown. In the present study, we provide evidence for the first time that upregulated miR-30b likely is an important mechanism responsible for synaptic dysfunction in AD.

It has been estimated that protein-coding genes only make up a <2% of the genome, indicating that most of the genome are transcribed into non-coding RNAs [7,56]. Research over the past two decades reveals non-coding miRNAs in regulation of cell function under normal and disease states. While miRNAs have been implicated in neurodegenerative diseases [8–17], previous studies primarily focused on Aβ production (e.g., targeting BACE1) [18–21]. However, AD at its early stage is synaptic failure [1–4,55]. To this end, we searched miRNAs that target the molecules important for synapses in our miRNA microarray screening [20] and found that expression of miR-30b, which has binding sites in the 3′UTRs' of sirt1, ephB2, and GluA2, is robustly elevated. The elevated expression of miR-30b is also confirmed in postmortem hippocampal tissues of AD patients. Elevated miR-30b results in repressing miR-30b targets, including sirt1, ephB2, and GluA2 in the hippocampi of both AD patients and TG mice. It has been proposed that a single miRNA may regulate many mRNAs as its targets, while a single molecule can be targeted by several miRNAs [6]. Therefore, the results showing that sirt1, ephB2, and GluA2 are regulated by miR-30b provide evidence that a single miRNA can regulate multiple targets.

EphB2 is a member of receptor tyrosine kinases and has been shown to play important roles in synaptogenesis, axon guidance, dendritic spine formation and synaptic maturation, AMPA and NMDA glutamate receptor expression and function, and long-term synaptic plasticity [44–47,57–59]. Sirt1 is an NAD-dependent deacetylase and has been long recognized to have protective effects against age-related diseases, including AD [60–63] and participate in regulation of axonal elongation,
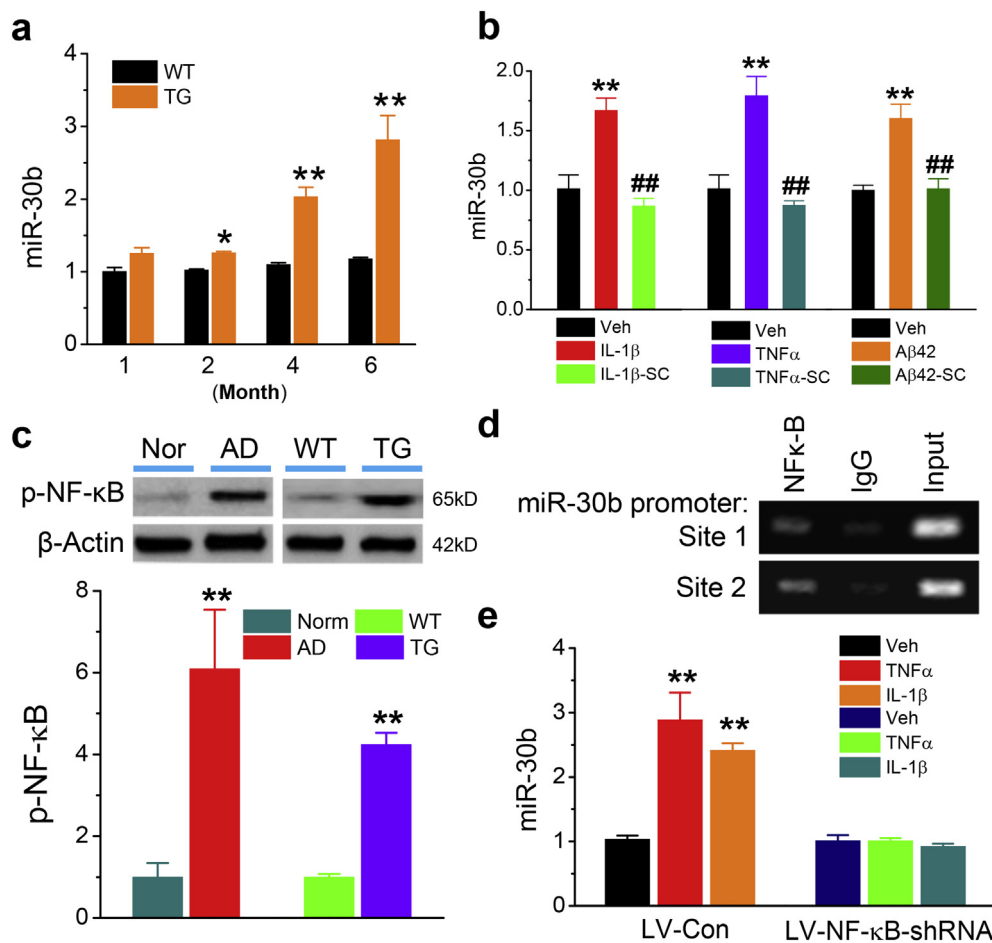
Fig. 5. Expression of miR-30b in the brain is triggered by neuroinflammation and regulated by NF-κB signaling pathway. (a) Age-dependent elevation of miR-30b expression in TG mice (ANOVA with Fisher's PLSD test, n = 3/group, *P < 0.05, **P < 0.01 compared with WT mice at one-month-old, n = 3/group). (b) Expression of miR-30b is upregulated by proinflammatory cytokines IL-1β (10 ng/ml), TNFα (10 ng/ml) or Aβ (10 μM) in cultured hippocampal neurons and the upregulation is blocked by SC-514 (SC, 100 μM). ANOVA with Fisher's PLSD test, ** < 0.01, compared with the vehicle control, ##P < 0.01 compared with Aβ, IL-1β, or TNFα (n = 3/group). (c) Increased phosphorylated NF-κB in the hippocampi of both AD patients and TG mice. Student's t-test, ** < 0.01, compared with normal subjects or WT controls (n = 4/group for human samples and n = 10/group for mouse samples). (d) Binding of the NF-κB p65 subunit in the promoter of the miR-30b gene assessed by chromatin immunoprecipitation (CHIP) analysis. (e) Silencing of the NF-κB p65 subunit blocks cytokines-induced increase in expression of miR-30b. Hippocampal neurons in culture were transfected with lentiviral vectors expressing control or NF-κB p65 shRNA (ANOVA with Fisher's PLSD test, ** < 0.01, compared with the vehicle control, n = 3/group with duplicates).
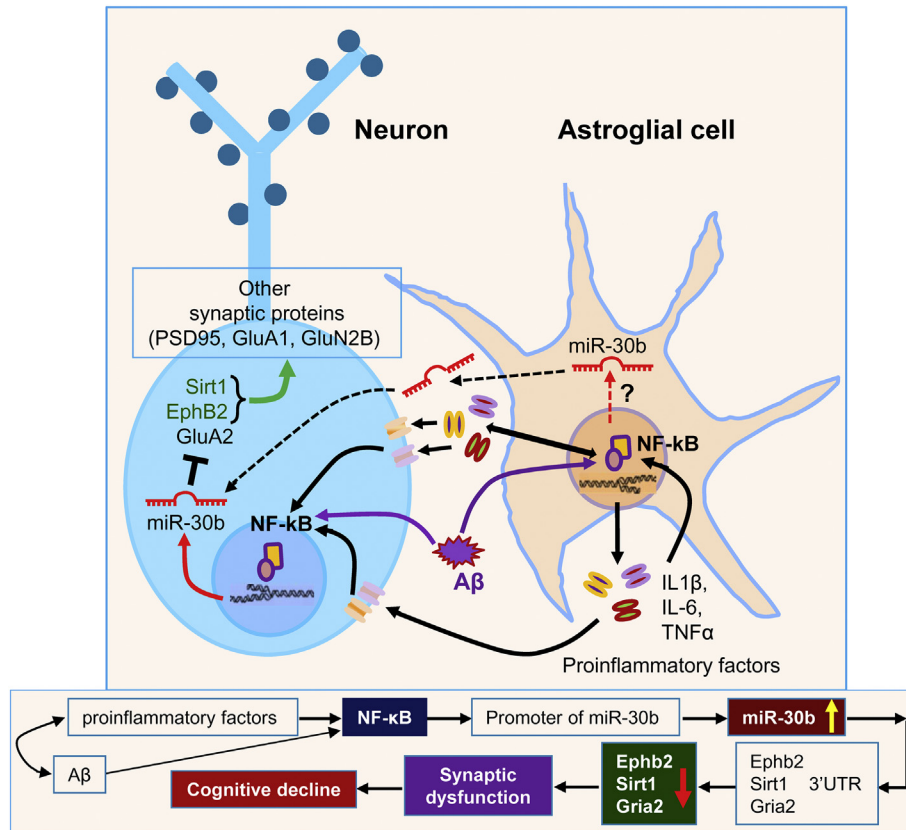
Fig. 6. Hypothetical signaling pathways involved in neuroinflammation triggered-upregulation of miR-30b that contributes to synaptic and cognitive deficits in AD.

neurite outgrowth, and dendritic branching, synaptic plasticity and memory formation [50,62,64]. Sirt1 also displays effects in reductions of cell death, Aβ formation, tau acetylation and phosphorylation, neuroinflammation, and NF-κB activity [60,65,66]. Therefore, the reduced density of dendritic spines and expression of glutamate receptor subunits GluA1 and GluN2B as well as PSD-95 in the hippocampus in WT mice that received LV-miR-30b and in TG mice we observed in the present study are likely associated with elevated expression of miR-30b, which represses ephB2 and sirt1. In fact, it has been shown previously that the levels of ephB2 and sirt1 in the brain and circulation are reduced in patients with mild cognitive impairment (MCI) and AD as well as in mouse models of AD [58,63,67,68], suggesting that reduced ephB2 and sirt1 in AD are likely attributed to the upregulated miR-30b. Previous studies demonstrated that overexpression of ephB2 alone is sufficient to rescue synaptic function and ameliorates learning and memory deficits in TG mice [44]. In addition, GluA2 is a subunit of the glutamate AMPA receptor, which is important for synaptic transmission and plasticity. Previous studies demonstrated that GluA2 is regulated by miR-124, which is important for social behaviors [69]. Therefore, impaired hippocampal basal synaptic transmission and LTP as well as learning and memory by overexpression of miR-30b in WT mice and upregulated miR-30b in TG mice likely result from the repression of miR-30b targets ephB2, sirt1 and GluA2. Improved long-term synaptic plasticity, learning and memory by knockdown of endogenous miR-30b, which leads to recovery of ephB2, sirt1 and GluA2 in TG mice, provide further evidence supporting the idea that upregulated miR-30b causes synaptic and cognitive dysfunction in AD. This speculation is also supported by the results showing that reduced density of dendritic spines and expression of glutamate receptor subunits GluA1 and GluN2B as well as PSD-95 are returned to normal control levels by knockdown of miR-30b in TG mice. Since GluA1, GluN2B and PSD-95 are not direct targets of miR-30b, changes in expression of these molecules are likely mediated by ephB2 and sirt1. Interestingly, while synaptic and cognitive functions are significantly improved by sequestration of miR-30b in TG mice, production of Aβ and expression of the enzymes synthesizing Aβ are not altered in these mice, suggesting that changes in the levels of miR-30b and its target molecules are not associated Aβ processing and that abnormally elevated expression of miR-30b would be the key issue that causes synaptic dysfunction in AD. These findings also suggest that maintaining the integrity of or improving synaptic function would be the key for AD therapies, especially, the information from the latest clinical trials indicates that anti-Aβ therapies do not significantly improve clinical outcomes in patients with mild-to-moderate AD [70–72].

Although it has been reported that several miRNAs are dysregulated in neurodegenerative diseases, it is largely unclear how miRNAs are dysregulated in the development of AD pathogenesis. Neuroinflammation has long been believed to contribute to the pathogenesis and neuropathology of AD [52–54]. We hypothesized that upregulation of miR-30 in AD may be triggered by neuroinflammatory responses. To this end, we explored the involvement of neuroinflammatory response in regulation of miR-30b transcription and expression. Our results show that miR-30b is upregulated by proinflammatory cytokines and Aβ, which activate NF-κB [20,32–34], and that NF-κB p65 displays binding activities in the promoter regions of the miR-30b gene. In particular, inhibition of NF-κB signaling pathway or silencing NF-κB p65 prevents cytokine-induced elevation of miR-30b. Previous studies demonstrate that NF-κB activity is increased in the brain of AD patients [73,74]. In the present study, we confirmed that NF-κB activity is increased in the brain of both AD patients and TG mice, suggesting that a steady upregulation of miR-30b expression triggered by chronic neuroinflammation is mediated through NF-κB signaling in AD (Fig. 6).

Overall, our study reveals a previously undefined mechanism by showing that overexpression of miR-30b (gin-of-function) in the hippocampus impairs hippocampal synaptic structure and function, which in turn, contributes to deficits in cognitive function in normal WT animals,

mimicking those seen in AD. Conversely, knockdown of endogenous miR-30b (loss-of-function) by miR-30b sequestration ('sponging') alleviates deficits in synaptic and cognitive function in TG mice. We should mention it here that many factors may contribute to synaptic failure in AD. However, a robustly elevated expression of miR-30b in the brains of both AD patients and TG mice suggests that impaired synaptic transmission and plasticity in AD are, at least, associated with repression of ephB2, sirt1 and GluA2 by miR-30b and that suppression or reversal of dysregulated miR-30b may mitigate or slow synaptic and cognitive deficits in AD.

Supplementary data to this article can be found online at https://doi.org/10.1016/j.ebiom.2018.11.059.

Conflict of interest

The authors declare no conflict of interest.

Acknowledgements

Author Contributions

Y.S., J.Z., M.H., Z-Q.T., and C.C. designed and performed the experiments and analyzed the data; C.C. conceived the project, supervised the work, and wrote the manuscript.

References

[1] Dekosky ST, Scheff SW. Synapse loss in frontal cortex biopsies in Alzheimer's disease: correlation with cognitive severity. Ann Neurol 1990;27(5):457–64.
[2] Selkoe DJ. Alzheimer's disease is a synaptic failure. Science 2002;298(5594):789–91.
[3] Forner S, Baglietto-Vargas D, Martini AC, Trujillo-Estrada L, Laferla FM. Synaptic impairment in Alzheimer's Disease: A dysregulated symphony. Trends Neurosci 2017; 40(6):347–57.
[4] Sheng M, Sabatini BL, Sudhof TC. Synapses and Alzheimer's disease. Cold Spring Harbor perspectives in biology, 4(5); 2012.
[5] Lepeta K, Lourenco MV, Schweitzer BC, Martino Adami PV, Banerjee P, Catuara-Solarz S, et al. Synaptopathies: synaptic dysfunction in neurological disorders - a review from students to students. J Neurochem 2016;138(6):785–805.
[6] Bartel DP. MicroRNAs: Target recognition and regulatory functions. Cell 2009;136 (2):215–33.
[7] Mehler MF, Mattick JS. Non-coding RNAs in the nervous system. J Physiol 2006;575 (Pt 2):333–41.
[8] Delay C, Mandemakers W, Hebert SS. MicroRNAs in Alzheimer's disease. Neurobiol Dis 2012;46(2):285–90.
[9] Satoh J. MicroRNAs and their therapeutic potential for human diseases: Aberrant microRNA expression in Alzheimer's disease brains. J Pharmacol Sci 2010;114(3): 269–75.
[10] Tan L, Yu JT, Hu N, Tan L. Non-coding RNAs in Alzheimer's disease. Mol Neurobiol 2013;47(1):382–93.
[11] Quinlan S, Kenny A, Medina M, Engel T, Jimenez-Mateos EM. MicroRNAs in neurodegenerative diseases. Int Rev Cell Mol Biol 2017;334:309–43.
[12] Banzhaf-Strathmann J, Benito E, May S, Arzberger T, Tahirovic S, Kretzschmar H, et al. MicroRNA-125b induces tau hyperphosphorylation and cognitive deficits in Alzheimer's disease. EMBO J 2014;33(15):1667–80.
[13] Lau P, de Strooper B. Dysregulated microRNAs in neurodegenerative disorders. Semin Cell Dev Biol 2010;21(7):768–73.
[14] Maes OC, Chertkow HM, Wang E, Schipper HM. MicroRNA: Implications for Alzheimer disease and other human CNS disorders. Curr Genomics 2009;10(3): 154–68.
[15] Qiu L, Tan EK, Zeng L. microRNAs and neurodegenerative diseases. Adv Exp Med Biol 2015;888:85–105.
[16] Abe M, Bonini NM. MicroRNAs and neurodegeneration: Role and impact. Trends Cell Biol 2013;23(1):30–6.
[17] Salta E, De Strooper B. Noncoding RNAs in neurodegeneration. Nat Rev Neurosci 2017;18:627–40.
[18] Hebert SS, Horre K, Nicolai L, Papadopoulou AS, Mandemakers W, Silahtaroglu AN, et al. Loss of microRNA cluster miR-29a/b-1 in sporadic Alzheimer's disease correlates with increased BACE1/beta-secretase expression. Proc Natl Acad Sci U S A 2008;105(17):6415–20.
[19] Wang WX, Rajeev BW, Stromberg AJ, Ren N, Tang G, Huang Q, et al. The expression of microRNA miR-107 decreases early in Alzheimer's disease and may accelerate disease progression through regulation of beta-site amyloid precursor protein-cleaving enzyme 1. J Neurosci 2008;28(5):1213–23.
[20] Zhang J, Hu M, Teng Z, Tang YP, Chen C. Synaptic and cognitive improvements by inhibition of 2-AG metabolism are through upregulation of microRNA-188-3p in a mouse model of Alzheimer's disease. J Neurosci 2014;34(45):14919–33.
[21] Boissonneault V, Plante I, Rivest S, Provost P. MicroRNA-298 and microRNA-328 regulate expression of mouse beta-amyloid precursor protein-converting enzyme 1. J Biol Chem 2009;284(4):1971–81.
[22] Cohen JE, Lee PR, Chen S, Li W, Fields RD. MicroRNA regulation of homeostatic synaptic plasticity. Proc Natl Acad Sci U S A 2011;108(28):11650–5.
[23] Edbauer D, Neilson JR, Foster KA, Wang CF, Seeburg DP, Batterton MN, et al. Regulation of synaptic structure and function by FMRP-associated microRNAs miR-125b and miR-132. Neuron 2010;65(3):373–84.
[24] Karr J, Vagin V, Chen K, Ganesan S, Olenkina O, Gvozdev V, et al. Regulation of glutamate receptor subunit availability by microRNAs. J Cell Biol 2009;185(4):685–97.
[25] McNeill E, Van Vactor D. MicroRNAs shape the neuronal landscape. Neuron 2012;75 (3):363–79.
[26] Rajasethupathy P, Fiumara F, Sheridan R, Betel D, Puthanveettil SV, Russo JJ, et al. Characterization of small RNAs in Aplysia reveals a role for miR-124 in constraining synaptic plasticity through CREB. Neuron 2009;63(6):803–17.
[27] Schratt G. microRNAs at the synapse. Nat Rev Neurosci 2009;10(12):842–9.
[28] Liu D, Tang H, Li XY, Deng MF, Wei N, Wang X, et al. Targeting the HDAC2/HNF-4A/miR-101b/AMPK pathway rescues tauopathy and dendritic abnormalities in Alzheimer's disease. Mol Ther 2017;25(3):752–64.
[29] Wang X, Liu D, Huang HZ, Wang ZH, Hou TY, Yang X, et al. A novel microRNA-124/PTPN1 signal pathway mediates synaptic and memory deficits in Alzheimer's disease. Biol Psychiatry 2018;83(5):395–405.
[30] Oakley H, Cole SL, Logan S, Maus E, Shao P, Craft J, et al. Intraneuronal beta-amyloid aggregates, neurodegeneration, and neuron loss in transgenic mice with five familial Alzheimer's disease mutations: Potential factors in amyloid plaque formation. J Neurosci 2006;26(40):10129–40.
[31] Chen R, Zhang J, Fan N, Teng ZQ, Wu Y, Yang H, et al. Delta9-THC-caused synaptic and memory impairments are mediated through COX-2 signaling. Cell 2013;155 (5):1154–65.
[32] Chen X, Zhang J, Chen C. Endocannabinoid 2-arachidonoylglycerol protects neurons against beta-amyloid insults. Neuroscience 2011;178:159–68.
[33] Du H, Chen X, Zhang J, Chen C. Inhibition of COX-2 expression by endocannabinoid 2-arachidonoylglycerol is mediated via PPAR-gamma. Br J Pharmacol 2011;163(7): 1533–49.
[34] Zhang J, Chen C. Endocannabinoid 2-arachidonoylglycerol protects neurons by limiting COX-2 elevation. J Biol Chem 2008;283(33):22601–11.
[35] Sang N, Zhang J, Marcheselli V, Bazan NG, Chen C. Postsynaptically synthesized prostaglandin E2 (PGE2) modulates hippocampal synaptic transmission via a presynaptic PGE2 EP2 receptor. J Neurosci 2005;25(43):9858–70.
[36] Zhang J, Teng Z, Song Y, Hu M, Chen C. Inhibition of monoacylglycerol lipase prevents chronic traumatic encephalopathy-like neuropathology in a mouse model of repetitive mild closed head injury. J Cereb Blood Flow Metab 2015; 35(3):443–53.
[37] Chen R, Zhang J, Wu Y, Wang D, Feng G, Tang YP, et al. Monoacylglycerol lipase is a therapeutic target for Alzheimer's disease. Cell Rep 2012;2(5):1329–39.
[38] He H, Mahnke AH, Doyle S, Fan N, Wang CC, Hall BJ, et al. Neurodevelopmental role for VGLUT2 in pyramidal neuron plasticity, dendritic refinement, and in spatial learning. J Neurosci 2012;32(45):15886–901.
[39] Silahtaroglu AN. LNA-FISH for detection of microRNAs in frozen sections. Methods Mol Biol 2010;659:165–71.
[40] Chen C, Magee JC, Bazan NG. Cyclooxygenase-2 regulates prostaglandin E2 signaling in hippocampal long-term synaptic plasticity. J Neurophysiol 2002;87(6):2851–7.
[41] Chen C. ZD7288 inhibits postsynaptic glutamate receptor-mediated responses at hippocampal perforant path-granule cell synapses. Eur J Neurosci 2004;19(3): 643–9.
[42] Chen C. beta-Amyloid increases dendritic Ca2+ influx by inhibiting the A-type K+ current in hippocampal CA1 pyramidal neurons. Biochem Biophys Res Commun 2005;338(4):1913–9.
[43] Leger M, Quiedeville A, Bouet V, Haelewyn B, Boulouard M, Schumann-Bard P, et al. Object recognition test in mice. Nat Protoc 2013;8(12):2531–7.
[44] Cisse M, Halabisky B, Harris J, Devidze N, Dubal DB, Sun B, et al. Reversing EphB2 depletion rescues cognitive functions in Alzheimer model. Nature 2011;469(7328): 47–52.
[45] Contractor A, Rogers C, Maron C, Henkemeyer M, Swanson GT, Heinemann SF. Trans-synaptic Eph receptor-ephrin signaling in hippocampal mossy fiber LTP. Science 2002;296(5574):1864–9.
[46] Henderson JT, Georgiou J, Jia Z, Robertson J, Elowe S, Roder JC, et al. The receptor tyrosine kinase EphB2 regulates NMDA-dependent synaptic function. Neuron 2001;32 (6):1041–56.
[47] Henkemeyer M, Itkis OS, Ngo M, Hickmott PW, Ethell IM. Multiple EphB receptor tyrosine kinases shape dendritic spines in the hippocampus. J Cell Biol 2003;163(6): 1313–26.
[48] McClelland AC, Hruska M, Coenen AJ, Henkemeyer M, Dalva MB. Trans-synaptic EphB2-ephrin-B3 interaction regulates excitatory synapse density by inhibition of postsynaptic MAPK signaling. Proc Natl Acad Sci U S A 2010;107(19):8830–5.
[49] Herskovits AZ, Guarente L. SIRT1 in neurodevelopment and brain senescence. Neuron 2014;81(3):471–83.

[50] Michan S, Li Y, Chou MM, Parrella E, Ge H, Long JM, et al. SIRT1 is essential for normal cognitive function and synaptic plasticity. J Neurosci 2010;30(29):9695–707.

[51] Ebert MS, Neilson JR, Sharp PA. MicroRNA sponges: Competitive inhibitors of small RNAs in mammalian cells. Nat Methods 2007;4(9):721–6.

[52] Heneka MT, Carson MJ, El Khoury J, Landreth GE, Brosseron F, Feinstein DL, et al. Neuroinflammation in Alzheimer's disease. Lancet Neurol 2015;14(4):388–405.

[53] Morales I, Guzman-Martinez L, Cerda-Troncoso C, Farias GA, Maccioni RB. Neuroinflammation in the pathogenesis of Alzheimer's disease. A rational framework for the search of novel therapeutic approaches. Front Cell Neurosci 2014;8:112.

[54] McGeer PL, Rogers J, McGeer EG. Inflammation, antiinflammatory agents, and Alzheimer's disease: the last 22 years. J Alzheimers Dis 2016;54(3):853–7.

[55] Nistico R, Pignatelli M, Piccinin S, Mercuri NB, Collingridge G. Targeting synaptic dysfunction in Alzheimer's disease therapy. Mol Neurobiol 2012;46(3):572–87.

[56] Pheasant M, Mattick JS. Raising the estimate of functional human sequences. Genome Res 2007;17(9):1245–53.

[57] Nolt MJ, Lin Y, Hruska M, Murphy J, Sheffler-Colins SI, Kayser MS, et al. EphB controls NMDA receptor function and synaptic targeting in a subunit-specific manner. J Neurosci 2011;31(14):5353–64.

[58] Sloniowski S, Ethell IM. Looking forward to EphB signaling in synapses. Semin Cell Dev Biol 2012;23(1):75–82.

[59] Tolias KF, Bikoff JB, Kane CG, Tolias CS, Hu L, Greenberg ME. The Rac1 guanine nucleotide exchange factor Tiam1 mediates EphB receptor-dependent dendritic spine development. Proc Natl Acad Sci U S A 2007;104(17):7265–70.

[60] Bonda DJ, Lee HG, Camins A, Pallas M, Casadesus G, Smith MA, et al. The sirtuin pathway in ageing and Alzheimer disease: mechanistic and therapeutic considerations. Lancet Neurol 2011;10(3):275–9.

[61] Donmez G, Outeiro TF. SIRT1 and SIRT2: emerging targets in neurodegeneration. EMBO Mol Med 2013;5(3):344–52.

[62] Gao J, Wang WY, Mao YW, Graff J, Guan JS, Pan L, et al. A novel pathway regulates memory and plasticity via SIRT1 and miR-134. Nature 2010;466(7310):1105–9.

[63] Kumar R, Chaterjee P, Sharma PK, Singh AK, Gupta A, Gill K, et al. Sirtuin1: A promising serum protein marker for early detection of Alzheimer disease. PLoS One 2013;8(4):e61560.

[64] Guo W, Qian L, Zhang J, Zhang W, Morrison A, Hayes P, et al. Sirt1 overexpression in neurons promotes neurite outgrowth and cell survival through inhibition of the mTOR signaling. J Neurosci Res 2011;89(11):1723–36.

[65] Min SW, Sohn PD, Cho SH, Swanson RA, Gan L. Sirtuins in neurodegenerative diseases: An update on potential mechanisms. Front Aging Neurosci 2013;5:53.

[66] Min SW, Cho SH, Zhou Y, Schroeder S, Haroutunian V, Seeley WW, et al. Acetylation of tau inhibits its degradation and contributes to tauopathy. Neuron 2010;67(6):953–66.

[67] Lutz MI, Milenkovic I, Regelsberger G, Kovacs GG. Distinct patterns of sirtuin expression during progression of Alzheimer's disease. Neuromolecular Med 2014;16(2):405–14.

[68] Qu M, Jiang J, Liu XP, Tian Q, Chen LM, Yin G, et al. Reduction and the intracellular translocation of EphB2 in Tg2576 mice and the effects of beta-amyloid. Neuropathol Appl Neurobiol 2013;39(6):612–22.

[69] Gascon E, Lynch K, Ruan H, Almeida S, Verheyden JM, Seeley WW, et al. Alterations in microRNA-124 and AMPA receptors contribute to social behavioral deficits in frontotemporal dementia. Nat Med 2014;20(12):1444–51.

[70] Abushouk AI, Elmaraezy A, Aglan A, Salama R, Fouda S, Fouda R, et al. Bapineuzumab for mild to moderate Alzheimer's disease: a meta-analysis of randomized controlled trials. BMC Neurol 2017;17(1):66.

[71] Brody M, Liu E, Di J, Lu M, Margolin RA, Werth JL, et al. A phase II, randomized, double-blind, placebo-controlled study of safety, pharmacokinetics, and biomarker results of subcutaneous bapineuzumab in patients with mild to moderate Alzheimer's disease. J Alzheimers Dis 2016;54(4):1509–19.

[72] Gold M. Phase II clinical trials of anti-amyloid beta antibodies: When is enough, enough? Alzheimer's & dementia (New York, N Y) 3(3); 2017; 402–9.

[73] Lukiw WJ, Bazan NG. Strong nuclear factor-kappaB-DNA binding parallels cyclooxygenase-2 gene transcription in aging and in sporadic Alzheimer's disease superior temporal lobe neocortex. J Neurosci Res 1998;53(5):583–92.

[74] Terai K, Matsuo A, McGeer PL. Enhancement of immunoreactivity for NF-kappa B in the hippocampal formation and cerebral cortex of Alzheimer's disease. Brain Res 1996;735(1):159–68.